

# A Distributed Wireless Testbed for Plug-in Hybrid Electric Vehicle Control Algorithms

Ian Beil      Ian Hiskens

Department of Electrical Engineering and Computer Science  
University of Michigan  
Ann Arbor, MI  
Email: {ianbeil,hiskens}@umich.edu

**Abstract**—There is a desire within the scientific community to use the inherent storage capabilities of plug-in hybrid electric vehicle batteries to enable demand-side management in power systems, increasing the usability of variable generation such as wind and solar power. The potential advantages of increased grid control must be tempered against the harmful effects of charge/discharge cycles on car battery health as well as user constraints on maximum allowable charge time. This paper reviews past research on communication and control architectures for PHEV charging and proposes a novel testbed to allow physical testing of several of the proposed schemes.

## I. INTRODUCTION

Concerns about climate change due to global warming have spurred research and industry efforts aimed at reducing carbon emissions. To this end, automobile manufacturers have begun selling plug-in hybrid electric vehicles (PHEVs) that use onboard batteries to store energy, resulting in increased fuel economy. By charging their batteries through the electrical grid, PHEVs use less gasoline than conventional vehicles, and may enable the transportation sector to reduce the amount of carbon it produces.

A large population of PHEVs could present further benefits to the power system infrastructure through careful utilization of their inherent energy storage capabilities. A well coordinated PHEV fleet would allow system operators to perform demand-side management by turning the battery chargers on or off, expanding the controllability of the grid and facilitating an increase in the amount of non-dispatchable generation such as wind and solar that could be accommodated. Battery charging could also provide ancillary services such as frequency regulation and contingency reserves that have traditionally been served by generation units.

The potential advantages of increased PHEV penetration can only be realized with the installation of a sufficiently robust, secure, and effective communication and control architecture. Complicating matters is the reality that the benefits of PHEVs to a grid operator often run counter to those of the vehicle owner, who places constraints on the allowable charge time and seeks to maximize battery health by limiting charge/discharge cycles.

This material is based upon work supported by the Department of Energy under Award Number DE-PI0000012, through the Clean Energy Research Center - Clean Vehicle Consortium.

This paper introduces a novel testbed designed to assess the performance of PHEV charging schemes using various communication technologies and control architectures. Using hardware that simulates PHEV Li-ion battery loads as well as typical household loads such as refrigerators and other appliances, the testbed will provide a way to assess the efficacy of fully networked charging control strategies.

## II. RELATED WORK

A large research effort has been undertaken towards defining future communication protocols for the electrical grid. Work on communication schemes specifically for PHEV charging is presented in [10], which examines four possible topologies:

- **HomePlug**, a form of broadband over power line communication (BB PLC), utilizes the pre-existing grid as a communication platform by placing encoded information on top of the 60 Hz line frequency;
- **Zigbee**, or IEEE 802.15.4, is a mesh network designed for low-power sensor environments;
- **ZWave** is a low data-rate protocol used specifically for home automation applications;
- **Cellular Networks** provide long-range capabilities and are already widely deployed.

The research in [10] suggested that cellular encryption schemes are not as robust or secure as those used by the other three topologies. Simulations of one-way load-based charging algorithms found that network traffic on a 1000 car network was well below the throughput capabilities of any of the four proposed communication schemes, although grid-level benefits may not be realized until PHEV penetration reaches higher populations, necessitating larger future simulations.

A further study [4] examined another power line scheme:

- **Narrowband PLC**, which enjoys cheaper deployment than BB PLC by avoiding the costs of couplers at the distribution/transmission border, because the narrowband signal can penetrate the transformer (albeit with a noise penalty).

Powerline communication schemes face the challenge of needing to filter the harmonics generated by battery charger inverters, but the study concluded that NB PLC could also provide a feasible communication protocol.

Any communication scheme will have inherent delays within the network, and the effect of these on a power system

are examined in [9], which simulates a power system with large renewable energy penetration buffered by a PHEV fleet. As expected, larger pools of vehicles and shorter communication delays lead to reduced power fluctuations, underscoring the effects a communication network can have on power system performance.

A higher-level perspective of the PHEV charging problem is presented in [3], which analyzes the tradeoffs between accomplishing system-wide objectives and ensuring non-disruptive, consumer-acceptable performance. The paper determines that centralized control of millions of individual PHEV loads is infeasible, necessitating the use of either hierachal or distributed control in conjunction with some form of load aggregator, which would merge the information from a group of PHEVs into a single dispatchable load from the grid operator's perspective. Work in this area includes [6], in which a Virtual Power Plant is designed for aggregate demand on the order of thousands of PHEVs. This work finds that either cellular networks or cable internet are viable communication media, but assumes PLC is not sufficiently reliable for the application. Another study [12] proposes that aggregators take into account trip estimations, utility service data, and ancillary service pricing in order to achieve performance similar to that of other ancillary service providers.

Control strategies are further explored in [11], which determines that, given 30% PHEV penetration, uncoordinated charging of PHEVs can result in up to a 50% increase in peak load. Meanwhile, local control based only on information available to the individual household reduces peak load by 26-30%, and global control based on system-wide information contributes an additional 4% decrease in peak load, suggesting that the majority of the benefits may be realizable using less infrastructure-intensive distributed control.

Studies on the practicality of using PHEVs for grid support include [8], which tested the Vehicle-to-Grid (V2G) concept using a custom-built PHEV fleet. The experiments validated the feasibility of using PHEVs for ancillary services, provided a mechanism is put in place to remove a vehicle from the regulation pool when its state-of-charge (SOC) gets too high or low.

Maximizing PHEV owner satisfaction is examined in [1], where the authors optimize the charge timing to minimize both the cost of electricity and battery life degradation due to solid-electrolyte interphase film growth. This formulation results in charge patterns that differ significantly from schemes that optimize only one objective. The best results are obtained by charging during off-peak billing hours using a high-rate charger shortly before the next scheduled trip, although this may conflict with the driver's desire for a flexible departure time. Further work presented in [7] examines the tradeoffs between battery health, driver flexibility, and increased grid functionality by simulating a distributed multi-agent system that optimizes for  $CO_2$  reduction and grid stability, increasing the use of renewable generation sources in the simulated power system.



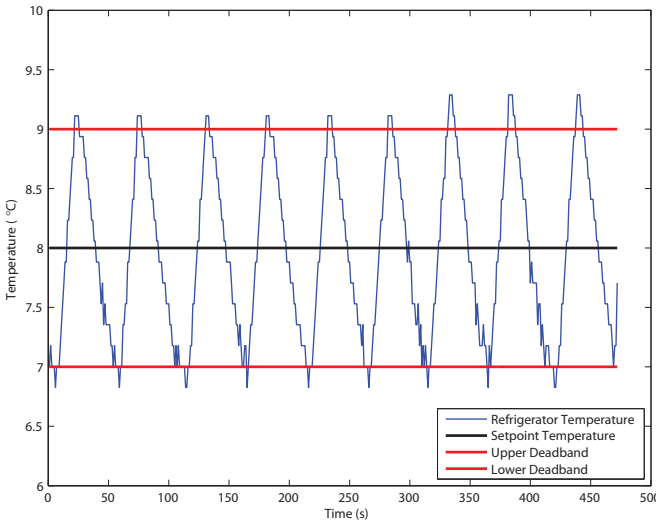


Fig. 2. Hysteresis-controlled refrigerator temperature during steady-state operation.

performance when the chargers enter constant-voltage mode.

The next component in the testbed is a hysteresis-controlled refrigerator. After purchasing a small residential refrigerator, the control equipment was gutted and replaced with a custom controller that enables remote sensing and actuation capabilities. The controller receives a temperature setpoint and deadband specifications from the server and uses hysteresis control to maintain the temperature within these bounds, as shown in Figure 2. It can also relay the power drawn by the refrigerator back to the server. This device is able to emulate the properties of other hysteresis-controlled loads such as air conditioners.

The last component in the testbed is a set of simple remote-controlled relays that plug into an outlet, allowing any 120V load to be attached. These devices represent typical household loads such as washers, dryers, or dishwashers that must be run at some point throughout the day, although the exact timing is not crucial. They receive commands from the server to turn on, but cannot be turned off until they have completed their task of a predetermined length.

Currently, communication is achieved through the use of XBee Series 2 Zigbee radios, which utilize the IEEE 802.15.4 Physical and Media Access Control layers and add the support of a Zigbee ad hoc, self-healing mesh network. Similar to work done in [2], these radios are operated in conjunction with Arduino Uno microcontroller boards, which provide both analog and digital I/O pins, streamlining data collection between the system components and the central server. The Arduinos possess enough onboard memory and computational power to implement the local control algorithms on a system component, such as the refrigerator's hysteretic control scheme, and to respond to signals from the server to increase or decrease power consumption. The system's modular design can also accommodate alternative forms of communication such as commercial HomePlug or ZWave transceivers, enabling the

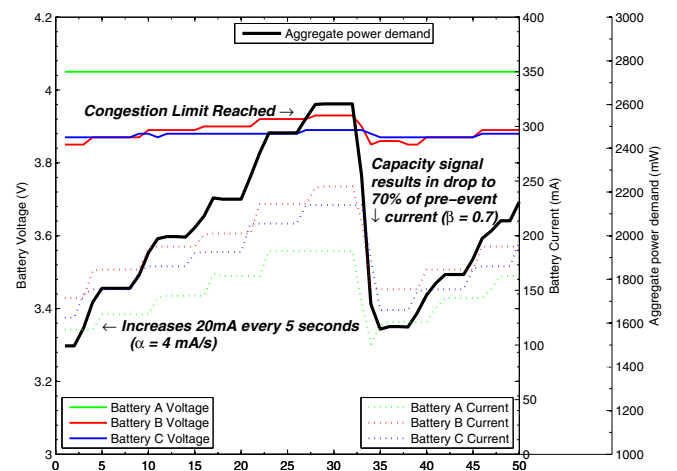


Fig. 3. Sample data from the testbed AIMD implementation, which shows the current limit for each charger stepping up at a rate  $\alpha$  until the 2500 mW global threshold is reached, at which time each charger reduces its current limit by a factor  $\beta$ .

comparison of communication topologies.

#### IV. AIMD IMPLEMENTATION AND RESULTS

Recent literature has proposed a variety of distributed algorithms designed to achieve coordination of PHEV charging. One such scheme presented in [13] considers the use of the Additive Increase Multiplicative Decrease (AIMD) algorithm, which is a well-studied technique for handling packet congestion on the internet. As a distributed algorithm, AIMD does not require local chargers to know anything about other chargers in the network, which greatly reduces system communication requirements. Furthermore, as pointed out in [13], the AIMD algorithm is robust in the presence of communication delays, which will be crucial for implementation using any of the proposed communication schemes.

The AIMD algorithm has two phases, as illustrated in Figure 3. During the Additive Increase phase, the local controller increases the usage rate of the global resource (in this case electrical power) at a constant rate  $\alpha$ . This continues until the local controller reaches its maximum power or the total available capacity of the global resource is exceeded. In this example, the total power capacity is constrained by the thermal limits of an imagined distribution transformer servicing the PHEV chargers. Reaching this limit triggers the Multiplicative Decrease phase, and the central controller transmits a signal telling all the local controllers to reduce their usage by a factor of  $\beta$ . It is worth noting that this scheme requires no communication from the local battery chargers to the central transformer, because the transformer simply observes its own load for a congestion limit. If that threshold is reached, the only communication required from the transformer to the chargers is a single piece of information indicating an occurrence of that event.

By adjusting the parameters  $\alpha$  and  $\beta$ , different system performance objectives can be realized. In order to compare the data acquired from the testbed to expected results, a simple

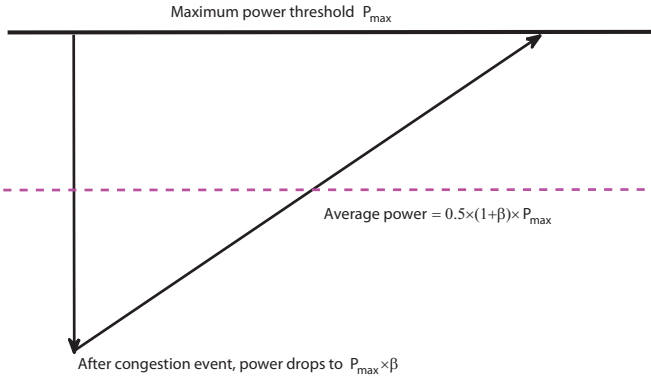


Fig. 4. Simple approximation for the average power delivered is based on  $\beta$  but not  $\alpha$ .

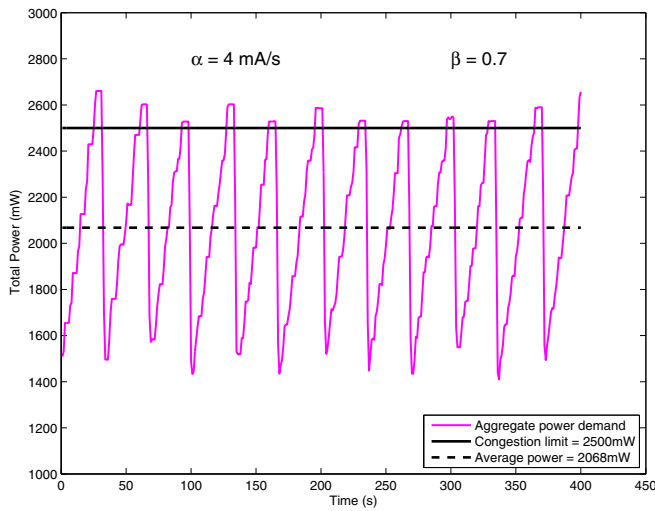


Fig. 5. Aggregate power demand under AIMD control,  $\alpha = 4$  mA/s,  $\beta = 0.7$ .

approximation is made for the average power delivered. As seen in Figure 4, when the maximum capacity is reached, the total power demand drops by a factor  $(1 - \beta)$ , and then ramps back up at a slope  $\alpha$ , forming a triangle with a vertical midpoint equal to the average power delivered. Since the midpoint is independent of the slope  $\alpha$ , only  $\beta$  affects the average power delivered, according to the formula

$$P_{avg} = \frac{1}{2}(1 + \beta) \times P_{max}.$$

Three tests were performed, with each test involving a three-PHEV setup and a maximum system power of 2500 mW. The first case used  $\alpha = 4$  mA/s and  $\beta = 0.7$ . Figure 3 shows measurements of the voltages, currents and aggregate power over a single cycle, while a longer view of the total power measurement is provided in Figure 5. The expected average power is  $P_{avg} = 2125$  mW, while the measured average power is 2068 mW.

In a second test, shown in Figure 6,  $\alpha$  was changed to 8 mA/s while  $\beta$  was left unchanged. The expected average power therefore remained the same. The measured average

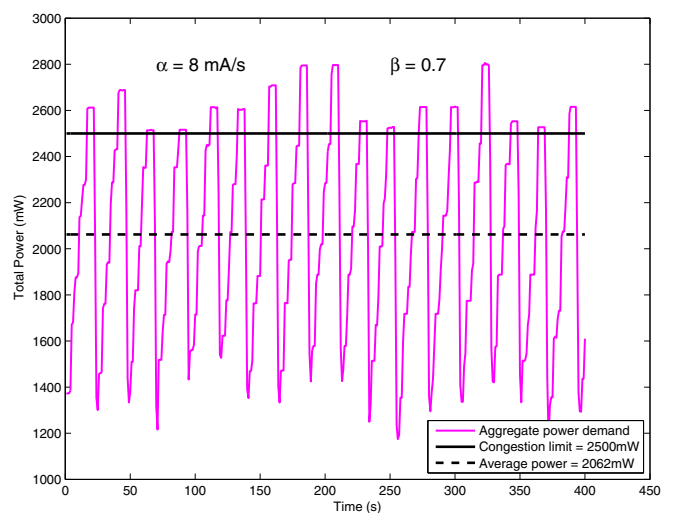


Fig. 6. Aggregate power demand under AIMD control,  $\alpha = 8$  mA/s,  $\beta = 0.7$ .

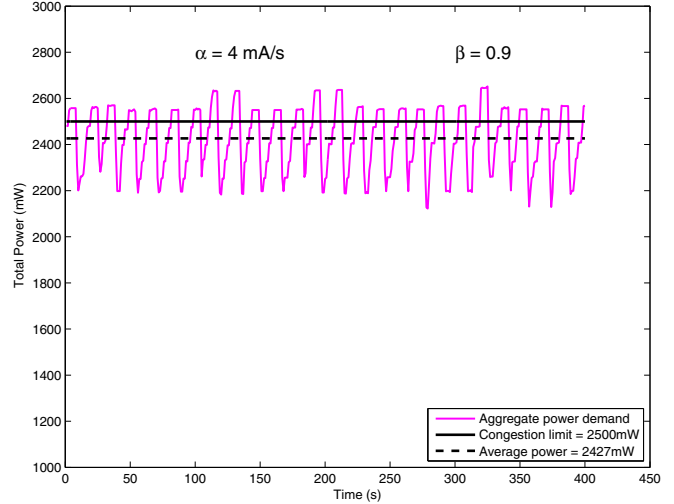


Fig. 7. Aggregate power demand under AIMD control,  $\alpha = 4$  mA/s,  $\beta = 0.9$ .

power in this case was 2062 mW, a very similar value to the first case and sufficiently close to the expected value to verify predicted behavior.

The third test kept  $\alpha = 4$  mA/s but used  $\beta = 0.9$ , with results displayed in Figure 7. In this case, the expected average power increased to 2375 mW, while the measured average power was 2427 mW. Again, this small difference suggested correct behavior of the algorithm.

It is also interesting to consider the situation where one or more of the chargers in the system switches from constant-current (CC) to constant-voltage (CV) mode. Since the maximum charge rate is constantly changing, the charger continually switches between CC and CV mode. Once the maximum possible current into the battery becomes much smaller than the other currents in the network, the load effectively ceases to undergo AIMD control and instead acts as a constant,

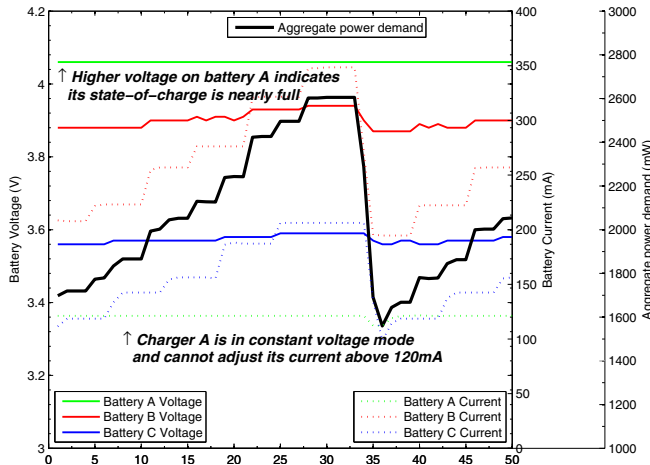


Fig. 8. Close up of AIMD control when a charger enters constant-voltage mode,  $\alpha = 4 \text{ mA/s}$ ,  $\beta = 0.9$ .

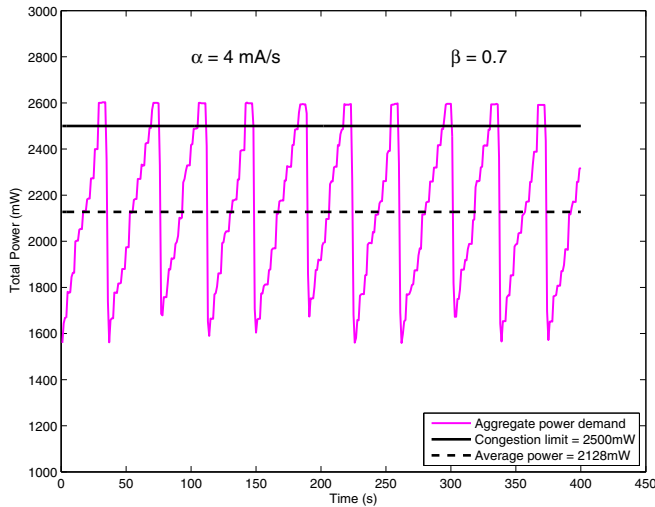


Fig. 9. Aggregate power demand with Charger A operating in constant-voltage mode,  $\alpha = 4 \text{ mA/s}$ ,  $\beta = 0.7$ .

uncontrollable load, as seen in Figure 8. However, because chargers enter CV mode near the end of the charging cycle, the amount of power they draw is relatively small at this point, and their effects on the system should be minimal.

Figure 9 displays the aggregate power while Charger A is in CV mode. The test was run with the same parameters as the first case,  $\alpha = 4 \text{ mA/s}$ ,  $\beta = 0.7$ , so the expected average power was again 2125 mW. The actual measured average power was 2128 mW. This value is higher than the first test case (with all chargers operating in CC mode) because Charger A does not reduce its load at all when the capacity signal is sent, so the total power stays closer to the maximum. Hence, at least from the point of view of maximizing the power delivered, chargers in CV mode should not diminish the overall performance of a system utilizing AIMD control.

## V. CONCLUSION

The demand flexibility inherent in the energy storage capability of a large, highly-distributed PHEV fleet can only be realized if the supporting communication and control architecture is well-designed. A large body of research has been dedicated to examining potential approaches to this challenge, but relatively little work has been undertaken to test these possibilities in hardware. The novel testbed presented in this paper was used to test the effectiveness of using the AIMD algorithm to control a set of constant-current constant-voltage chargers. Further work will examine the use of more complex AIMD related algorithms, as well as system performance in the presence of background loads such as household appliances. The testbed should allow experimentation on a variety of communication protocols and control schemes, offering a better understanding of the practicality of these architectures.

## REFERENCES

- [1] S. Bashash et al., *Plug-in hybrid electric vehicle charge pattern optimization for energy cost and battery longevity*, Journal of Power Sources **196** (2010), 541-549.
- [2] S.T. Cady, A.D. Dominguez-Garcia, and C.N. Hadjicostis, *Robust Implementation of Distributed Algorithms for Control of Distributed Energy Resources*, North American Power Symposium (2011).
- [3] D. Callaway and I. Hiskens, *Achieving Controllability of Electric Loads*, Proceedings of the IEEE **99** (Jan. 2011), no. 1, 184-199.
- [4] S. Galli, A. Scaglione, and Z. Wang, *Power Line Communications and the Smart Grid*, Proceedings of the International Conference on Smart Grid Communications (2010), 303-308.
- [5] R. Hermans, M. Almassalkhi, and I. Hiskens, *Incentive-based Coordinated Charging Control of Plug-in Electric Vehicles at the Distribution-Transformer Level*, Proceedings of the American Control Conference (June 2012).
- [6] B. Jansen, O. Sundstrom, and D. Gantenbein, *Architecture and Communication of an Electric Vehicle Virtual Power Plant*, Proceedings of the International Conference on Smart Grid Communications (2010), 149-154.
- [7] J. Keiser et al., *A Distributed Multi-Operator W2V2G Management Approach*, Proceedings of the International Conference on Smart Grid Communications (2011), 273-278.
- [8] W. Kempton et al., *A Test of Vehicle-to-Grid (V2G) for Energy Storage and Frequency Regulation in the PJM System*, University of Delaware V2G Project (Nov. 2008).
- [9] K.M. Liyange et al., *Impacts of Communication Delay on the Performance of a Control Scheme to Minimize Power Fluctuations Introduced by Renewable Generation under Varying V2G Vehicle Pool Size*, Proceedings of the International Conference on Smart Grid Communications (2010), 85-90.
- [10] T. Markel, M. Kuss, and P. Denholm, *Communication and Control of Electric Vehicles Supporting Renewables*, Proceedings of the IEEE Vehicle Power and Propulsion Systems Conference (Sep. 2009).
- [11] K. Mets et al., *Optimizing Smart Energy Control Strategies for Plug-In Hybrid Electric Vehicle Charging*, Proceedings of 1st IFIP/IEEE International Workshop on Management of Smart Grids (Apr. 2010), 293-299.
- [12] C. Quinn, D. Zimmerle, and T.H. Bradley, *The effect of communication architecture on the availability, reliability, and economics of plug-in hybrid electric vehicle-to-grid ancillary services*, Journal of Power Sources **195** (2010), 1500-1509.
- [13] S. Studli et al., *A flexible distributed framework for realising electric and plug-in hybrid vehicle charging policies*, International Journal of Control (Apr. 2012).